Ab initio structural and electronic properties of hydrogenated silicon nanoclusters in the ground and excited state

Elena Degoli,[1] G. Cantele,[2] Eleonora Luppi,[3] Rita Magri,[3] D. Ninno,[2] O. Bisi,[1] and Stefano Ossicini[1]
[1]*INFM-S*[3] *and Dipartimento di Scienze e Metodi dell'Ingegneria, Università di Modena e Reggio Emilia, via Fogliani, I-42100 Reggio Emilia, Italy*
[2]*INFM and Università di Napoli "Federico II" -Dipartimento di Scienze Fisiche, Complesso Universitario Monte S. Angelo, Via Cintia, I-80126 Napoli, Italy*
[3]*INFM-S*[3] *and Dipartimento di Fisica, Università di Modena e Reggio Emilia, via Campi 213/A, I-41100 Modena, Italy*
(Received 1 August 2003; revised manuscript received 31 October 2003; published 14 April 2004)

Electronic and structural properties of small hydrogenated silicon nanoclusters as a function of dimension are calculated from *ab initio* technique. The effects induced by the creation of an electron-hole pair are discussed in detail, showing the strong interplay between the structural and optical properties of the system. The distortion induced on the structure after an electronic excitation of the cluster is analyzed together with the role of the symmetry constraint during the relaxation. We point out how the overall effect is that of significantly changing the electronic spectrum if no symmetry constraint is imposed to the system. Such distortion can account for the Stokes shift and provides a possible structural model to be linked to the four-level scheme invoked in the literature to explain recent results for the optical gain in silicon nanoclusters. Finally, formation energies for clusters with increasing dimension are calculated and their relative stability discussed.

DOI: 10.1103/PhysRevB.69.155411 PACS number(s): 73.22.−f, 61.10.Ht, 78.55.Mb, 78.67.Bf

I. INTRODUCTION

The interest in studying (both experimentally and theoretically) semiconductor nanocrystals has significantly increased in the last years. The huge efforts done toward the matter manipulation down to nanometric scale have been motivated by the fact that desirable properties in the optical response, single-electron transport, etc. can be achieved and tuned by just changing the system size and shape as well as the atomic species which it contains.

The theoretical understanding of the physical aspects involved in size-dependent phenomena is not an easy task. Simple models such as effective-mass approximation have been demonstrated to be able to qualitatively and sometimes quantitatively account for size- and shape-dependent features.[1,2] Nevertheless, many studies have pointed out the need of a microscopic analysis, mostly for those aspects related to how the reduced size is reflected into the microscopic arrangement of atoms and/or molecules within the nanosystem.[3,4] Semiempirical tight-binding[5] and pseudopotential[6] calculations show that it is possible to overcome the intrinsic limits of continuous models like the effective-mass approximation, still considering large enough systems. On the other hand, *ab initio* approaches can be applied to smaller systems with the advantage of being parameter free. Theoretical investigations accounting for microscopic aspects have widely used density-functional theory (DFT) both within all-electron[7–11] and several pseudopotential schemes [local-density approximation (LDA),[12–15] time dependent density-functional theory (TDDFT),[16,17] quantum Monte Carlo techniques,[13,14,18] GW,[18,19] etc.]. The treatment of excited-state configurations within DFT is still a complex issue, mostly due to well-known problems arising when optical gaps are calculated. This explains why many aspects concerning the methods and the results obtained for excitation energies are still object of debate.[4,20,21] On the other hand, from an experimental point of view, large interest has been given to a wide range of applications which involve the nanosystem response under excitation. It is worth mentioning, among the many, the recently shown possibility of obtaining optical gain from silicon quantum dots.[22,23] The understanding of the physical mechanisms at the origin of this phenomenon implies the analysis of both the ground and excited state of the optically excited nanodots.

The theoretical study of phenomena such as the Stokes shift (difference between emission and absorption energies), the photoluminescence emission energy vs nanocrystals size, etc. can give a fundamental contribution to the understanding of the optical response of such systems. A lot of work has been done dealing with excited nanoclusters, but a clear comprehension of some aspects is still lacking. In this paper we present an analysis of hydrogenated silicon nanocrystals (H-Si-nc). The aim is that of investigating in a systematic way their structural, electronic, and stability properties as a function of both size and symmetry as well as pointing out the main changes induced by the nanocrystal excitation.

In Sec. II we give an outline of the method which our calculations are based on.

In Sec. III we focus on the structural properties, calculated for nanocrystals both in the ground- and in an excited-state configuration (corresponding to the first allowed optical transition) showing how the different electronic configurations can modify such structural properties.

In Sec. IV we show how the overall cluster structure is reflected into the electronic spectrum of the system. Again, we point out the main differences between ground- and excited-state configurations and try to explain the Stokes shift in terms of them. Furthermore, a four-level model for the optical gain in silicon nanocluster is discussed within this scheme.

In Sec. V we discuss the role played by symmetries in

relaxation studies. There are papers in the literature which do not pay attention to this aspect.[17,24] When structural optimization in the excited state is carried out it is essential to relax the ground-state symmetries in order to make the system free to evolve. This point will be emphasized by showing results obtained both keeping and relaxing the constraint on the cluster symmetry.

Finally, a calculation of the formation energy for different clusters is performed in Sec. VI, with the aim of addressing size-dependent features on the stability of such clusters. Since the formation energy is related to the hydrogen chemical potential, we also consider a cluster with some H passivating atoms missing, which gives rise to surface reconstruction with the formation of Si-Si dimers.[25,26]

II. METHOD AND DETAILS OF CALCULATION

The study of H-Si-nc has been done within the density functional theory, using a pseudopotential, plane-wave approach. All the calculations have been performed with the ABINIT code.[27] Norm-conserving, nonlocal Hamann-type pseudopotentials have been used. The Kohn-Sham wave functions have been expanded within a plane-wave basis set, choosing an energy cutoff of 32 Ry. The calculations performed are not spin polarized.[28] Each H-Si-nc has been embedded within a large cubic supercell, containing vacuum in order to make nanocrystal-nanocrystal interactions negligible. The supercell side has been fixed from 13.4 Å to 16.9 Å, according to the cluster dimension. Convergence with respect to both energy cutoff and supercell side has been checked. Gradient-corrected Perdew-Burke-Ernzerhof (GGA-PBE) exchange-correlation functional has been used for both structural and electronic states calculations. The pseudopotentials have been tested on bulk Si and H_2 molecule, giving equilibrium bond lengths of 2.366 Å and 0.744 Å, respectively, that should be compared with the experimental values 2.352 Å and 0.7414 Å.

The calculations for each cluster have been performed both in the ground and the excited state considering as the excited state the electronic configuration in which the highest occupied single-particle state (HOMO) contains a hole (h), while the lowest unoccupied single-particle state (LUMO) contains the corresponding electron (e). The structural properties have been determined by allowing full relaxation of each H-Si-nc until the maximum force was lower than 5×10^{-5} Ha/Bohr. The starting configuration for all the clusters but $Si_{29}H_{24}$ has been fixed with all Si atoms occupying the same position as in the bulk crystal, and passivating the surface with H atoms placed along the bulk crystal directions, at a distance determined by studying the SiH_4 molecule. For $Si_{29}H_{24}$ we remove twelve H atoms in such a way to induce surface reconstruction. This will be discussed in Sec. VI. It is worth pointing out that the starting H-Si-nc has T_d symmetry, which is kept during relaxation in the ground-state configuration. However, for excited-state configurations such a symmetry is generally lost, due to the occupation of excited energy levels. Therefore, for both the electronic configurations, we did the structural optimization both by keeping (see Sec. V) and relaxing (see Secs. III and IV) the constraint of T_d symmetry. The differences and the main results coming out in the two cases will be discussed in the following. We have verified that, starting from the distorted excited state geometry and going back down to the ground state the systems relax again to the T_d symmetric configuration suggesting that this should be a global minimum as supported also by the work of Meleshko *et al.*[30]

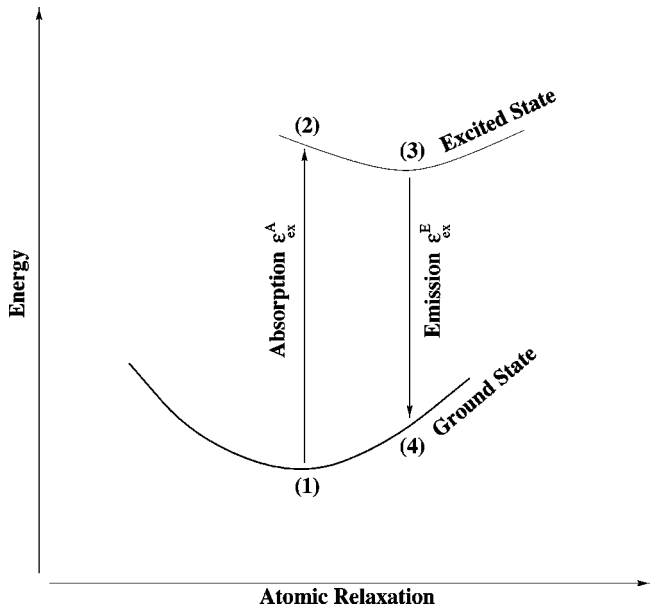

FIG. 1. Schematic representation of a Stokes shift relaxation. In position (1), the cluster is in its electronic ground state, and the atomic geometry is relaxed to its lowest energy configuration. On absorption of a photon, the nanocluster undergoes a vertical electronic excitation from (1) to (2). Once in the excited electronic state, the atomic geometry of the cluster relaxes to a lower energy configuration [from (2) to (3)]. Finally, the excited electron and hole recombine via another vertical transition, (3) to (4). The Stokes shift is defined as $\varepsilon_{ex}^{A}-\varepsilon_{ex}^{E}$.

The nanoclusters excitation has been studied calculating pair-excitation energies.[14,31] The formation of an electron-hole pair under excitation is taken into account forcing one electron to occupy the LUMO, thus leaving a hole in the HOMO. A schematic representation is drawn in Fig. 1. The nanocluster excitation [(1) to (2) in the figure] occurs with the atomic positions fixed in their ground-state configuration. Following Ref. 31, we indicate with $E(N,e\text{-}h)$ the total energy of the nanocluster calculated with the electron-hole pair constraint. The difference $\varepsilon_{ex}^{A}=E(N,e\text{-}h)-E(N)$ [$E(N)$ being the N-electron ground-state total energy] gives the energy needed for the creation of the pair, and defines the absorption edge [let us note that, with reference to Fig. 1, $E(N)\equiv E_1$ and $E(N,e\text{-}h)\equiv E_2$, E_1 and E_2 being the cluster total energies in the configuration 1 and 2, respectively]. It should be noted that the quasiparticle gap defined as $E(N+1)+E(N-1)-2E(N)$, and calculated from the $N+1$-, $N-1$- and N-electron total energies, neglects the effect of the Coulomb attraction between the electron and the hole; actually this gap is calculated starting from the energies needed to the creation of a hole and one electron separately.

After excitation, due to the change in the charge density,

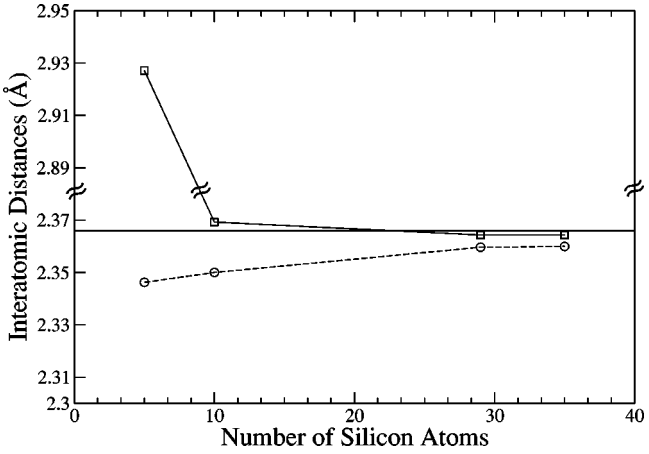

FIG. 2. Average Si-Si interatomic distances for the relaxed Si_5H_{12}, $Si_{10}H_{16}$, $Si_{29}H_{36}$, and $Si_{35}H_{36}$ clusters in their ground- (circle) and excited- (square) state configurations. The horizontal line indicates the calculated bulk Si interatomic distances.

relaxation occurs until the atoms reach a new minimum energy configuration, in presence of the electron-hole pair [(2) to (3) in the figure]. This modifies the electronic spectrum, implying that the levels involved in the emission process [electron-hole recombination, (3) to (4) in the figure] change. The emission energy can be defined as $\varepsilon_{ex}^{E}=E'(N,e\text{-}h)-E'(N)$, where $E'(N,e\text{-}h)$ and $E'(N)$ are the nanocluster total energies evaluated in presence and in absence of the electron-hole pair, respectively, with the atoms occupying the equilibrium positions of the excited state [see (3) and (4) in the figure, with $E'(N,e\text{-}h)\equiv E_3$, $E'(N)\equiv E_4$].

The difference $\Delta E^{Stokes}=(\varepsilon_{ex}^{A}-\varepsilon_{ex}^{E})$ [which, in Fig. 1, corresponds to $(E_2-E_1)-(E_3-E_4)$] defines the Stokes shift. Therefore, a contribution to the Stokes shift arises from relaxation after excitation of the nanocluster. This model assumes that the relaxation under excitation is faster than the electron-hole recombination.

III. STRUCTURAL PROPERTIES: GROUND STATE VERSUS EXCITED STATE

The structural properties of semiconductor nanoclusters have been calculated performing, for each cluster, a geometry optimization both in the ground- and excited-state configuration without any symmetry constraint. Symmetry considerations and related problems will be discussed in Sec. V. As previously said, we describe the excited-state configuration through an electron-hole pair, leaving a hole in the HOMO and forcing an electron in the LUMO. There are two interesting points which it is worth stressing here. The first one concerns the way in which the ground-state structural properties change as a function of the cluster dimension, while the second one is related to how the creation of an electron-hole pair modifies the overall structures. A contraction of the H-Si-nc in their ground state configuration with respect to bulk silicon is clearly shown in Fig. 2. Here the average Si-Si bond lengths of the relaxed Si_5H_{12}, $Si_{10}H_{16}$, $Si_{29}H_{36}$, and $Si_{35}H_{36}$ clusters in their ground- and excited-state configurations are reported as a function of the number

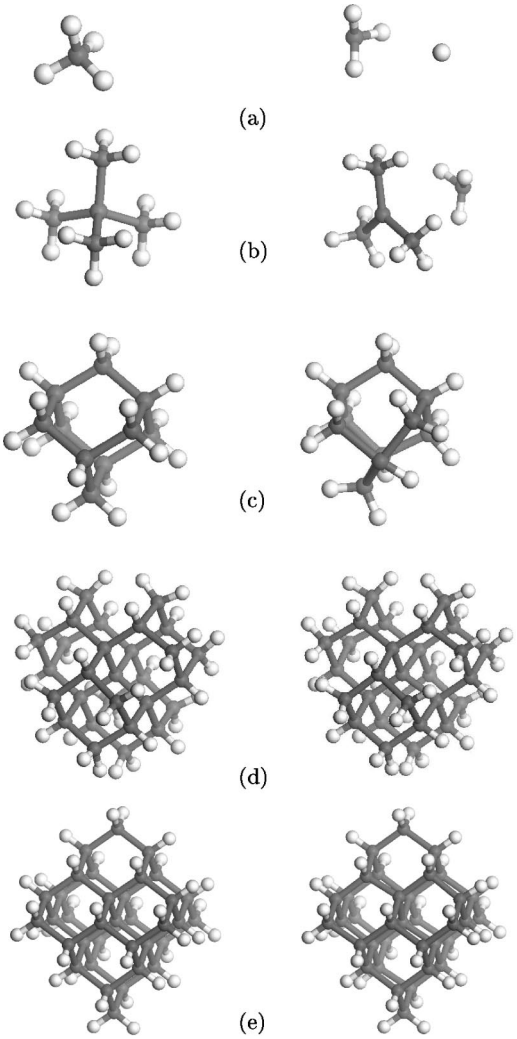

FIG. 3. Relaxed structures for the (a) Si_1H_4, (b) Si_5H_{12}, (c) $Si_{10}H_{16}$, (d) $Si_{29}H_{36}$, and (e) $Si_{35}H_{36}$ clusters calculated in the ground- (left panel) and excited-state (right panel) configuration.

of Si. The contraction becomes smaller and the average interatomic distances tend to the calculated bulk value as the size of the cluster increases. However, no clear trend can be identified for the excited-state configuration because of heavy clusters distortions that will be discussed in more detail later in this section. Similar results have been found in Ref. 24, which points out a contraction effect on the average bond lengths,[32] approaching the bulk value for H-Si-nc with diameter of about 20 Å as well as the absence of a uniform behavior for the excited structures. In order to better understand the overall contraction visible in Fig. 2 for the $Si_{29}H_{36}$ cluster, we have calculated the Si-Si bond lengths for each shell[33] and we have compared them with that calculated for bulk silicon. We have found a contraction of the outer silicon shells but a substantial agreement of the inner shells with the bulk.

We have also investigated the structural distortions caused by the nanocluster relaxation in the excited configuration. In order to qualitatively appreciate the structural changes, we have plotted in Fig. 3 the relaxed structures of some of the considered clusters, both in ground- and excited-state con-

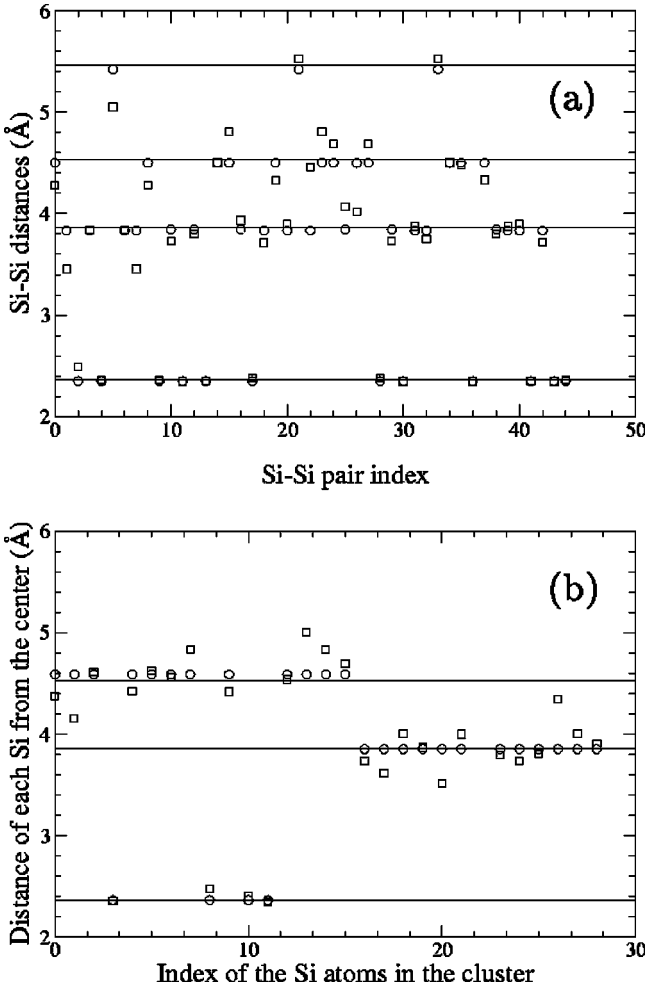

FIG. 4. Calculated Si-Si distances (a) for each pair of Si atoms for the $Si_{10}H_{16}$ cluster, (b) of each Si atom with respect to the central Si of the $Si_{29}H_{36}$ cluster. Circles and squares represent ground- and excited-state configurations, respectively. Straight lines represent calculated bulk silicon values for the first, second, third, and fourth neighbors distances.

figurations. The Si-H bond lengths remain practically unchanged for both the ground and excited state configurations, in contrast with the Si-Si distances (indicating that the excitation concerns the Si shells rather than being simply localized on the surface). This is shown in Fig. 4(a) for the $Si_{10}H_{16}$ cluster, for which we have studied the Si-Si distance for each pair of Si atoms (this cluster is centered in the vacuum and no ''central'' atom can be identified). The first-, second-, third-, and fourth-neighbor distances are almost unchanged, with respect to bulk values, in the ground-state configuration (circles) while significant deviations are induced by the excitation (squares). The same evidence comes from the analysis of the $Si_{29}H_{36}$ cluster [see Fig. 4(b)]. In this case, being the number of Si-Si pairs quite large we have chosen to show in particular the distances of each Si atom from the central one.[33] Therefore, the presence of an electron-hole pair in the clusters causes a strong deformation of the structures with respect to their ground-state configuration, and this is more evident for smaller systems. This is what we expect, since for large clusters the charge-density perturbation is distributed throughout the structure, and the effect locally induced becomes less evident (small adjustments of bonds and angles occur with respect to the ground state). On reducing the dimension, such effect can induce large distortions of the structure, which for Si_1H_4 and Si_5H_{12} are so strong that the clusters seem to break (see Fig. 3).[34]

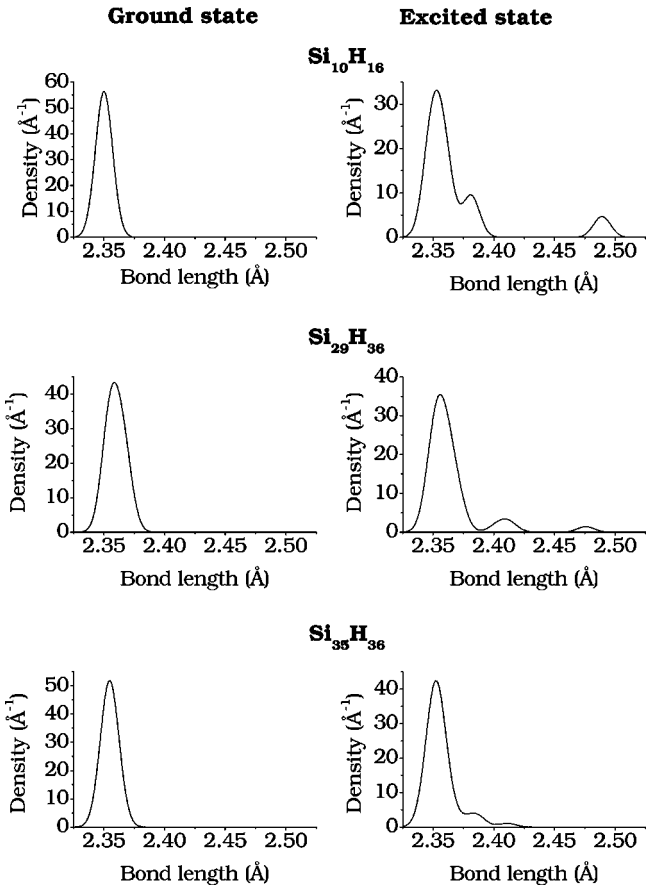

FIG. 5. Si-Si bond-length distribution in the ground- (left panel) and excited-state (right panel) geometries. The total area under each curve is normalized to one.

As a final check, following Ref. 29, we report in Fig. 5 the Si-Si bond-length distribution relative to Si_5H_{12}, $Si_{10}H_{16}$, $Si_{29}H_{36}$, and $Si_{35}H_{36}$ clusters. It is seen that, as the cluster dimension increases, the distortion induced on the structure by the excitation changes becoming less evident for large clusters. This agrees with the result of Franceschetti *et al.*,[29] which shows how under excitation the stretching of a single Si-Si bond is observed in small clusters, while on increasing the dimension the overall shape of the nanocrystal is changed (this last regime is clearly found for clusters with typical dimension much larger than ours).

IV. ELECTRONIC PROPERTIES

The structural modifications are immediately reflected into the electronic spectrum. In Fig. 6 we report the Kohn-Sham levels for the Si_5H_{12}, $Si_{10}H_{16}$, $Si_{29}H_{36}$, and $Si_{35}H_{36}$ clusters in both the ground- (left panel) and excited-state (right panel) configurations. It can be noted that: (i) the ground-state energy gap decreases on increasing the cluster

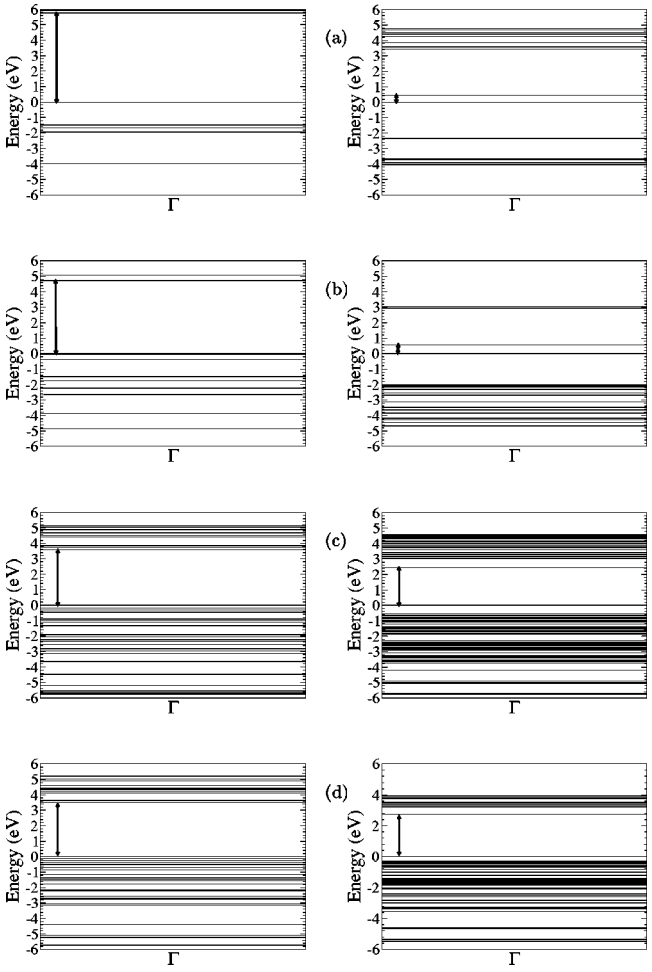

FIG. 6. Calculated energy levels at the Γ point for the (a) Si_5H_{12}, (b) $Si_{10}H_{16}$, (c) $Si_{29}H_{36}$, and (d) $Si_{35}H_{36}$ clusters in ground- (left) and excited- (right) state configuration. The energies are referred to the highest valence level.

dimension as expected; (ii) the excitation of the electron-hole pair causes a reduction of the energy gap which is more significant for smaller clusters.

For the excited clusters the HOMO and LUMO become strongly localized in correspondence of the distortion, giving rise to defectlike states which reduce the gap; these effects are stronger for smaller clusters. The contour plots[35] of the HOMO and LUMO wave functions (square modulus) confirm such a picture, as shown in Figs. 7 and 8 for the Si_5H_{12}, $Si_{10}H_{16}$, $Si_{29}H_{36}$, and $Si_{35}H_{36}$ clusters in the ground- and excited-state configurations, respectively. For $Si_{29}H_{36}$ our result is in accordance with that of Ref. 29, showing that the stretching induced by the excitation lies inside the nanocrystal, with the HOMO wave function localized around it.

The absorption of resonant radiation by the cluster in its ground-state configuration induces a transition between the HOMO and LUMO levels, which for all these clusters is optically allowed. Such a transition is followed by a cluster relaxation in the excited state configuration giving rise to distorted geometries (as shown in the previous section) and to new LUMO and HOMO, whose energy difference is smaller than that in the ground-state geometry (see Fig. 6). It

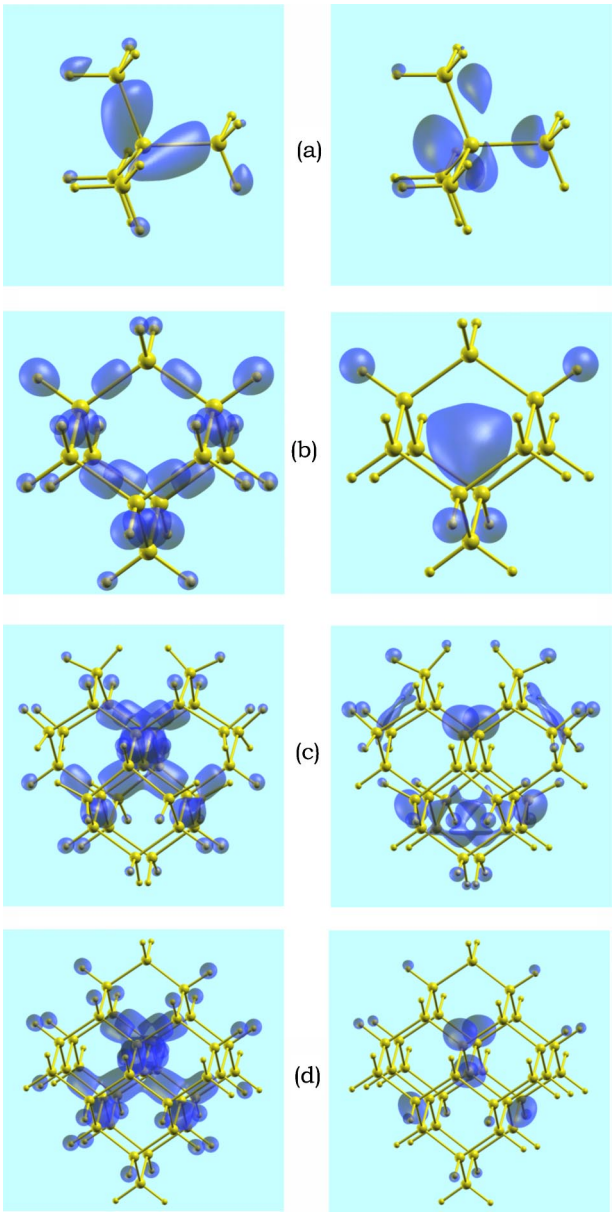

FIG. 7. (Color online) The HOMO (left panel) and LUMO (right panel) square modulus contour plots calculated for the (a) Si_5H_{12}, (b) $Si_{10}H_{16}$, (c) $Si_{29}H_{36}$, and (d) $Si_{35}H_{36}$ clusters in the ground-state configuration. The isosurfaces correspond to 25% of the maximum value. For $Si_{10}H_{16}$, $Si_{29}H_{36}$, and $Si_{35}H_{36}$ we get a threefold degenerate HOMO and the shown charge density is the sum over the three states.

is between these two last states that emission occurs and it is worth pointing out how such a shift changes as a function of the dimension. In Table I we show the HOMO-LUMO gap for both the ground and excited states together with the absorption and emission energies and the derived Stokes shift calculated as described in Sec. II. Let us recall that we calculate the absorption gap with the atoms fixed at the ground-state relaxed positions as the difference between the total energy of the cluster in presence of the electron-hole pair and the total energy in the ground-state configuration. The emission gap is calculated in a similar way, but with the relaxed geometry of the excited state.

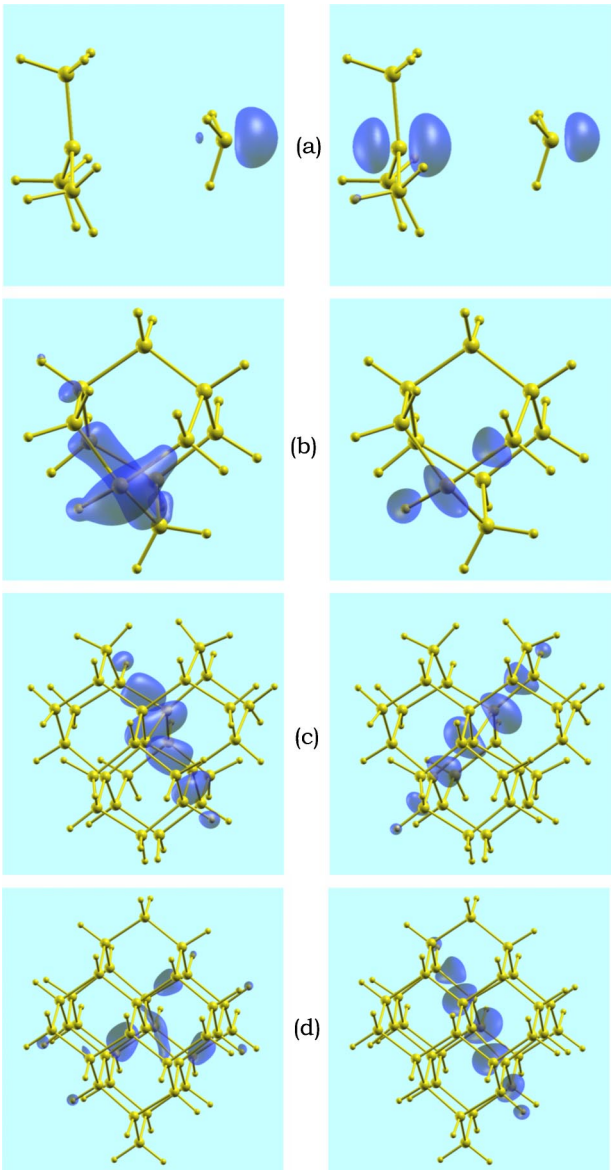

FIG. 8. (Color online) The HOMO (left panel) and LUMO (right panel) square modulus contour plots calculated for the (a) Si_5H_{12}, (b) $Si_{10}H_{16}$, (c) $Si_{29}H_{36}$, and (d) $Si_{35}H_{36}$ clusters in the excited-state configuration. The isosurfaces correspond to 25% of the maximum value.

A number of papers present in literature (for a recent review see Ref. 36) consider the HOMO-LUMO gaps of the ground and excited state as the proper absorption and emission energies; this leads to wrong results, mostly for the smaller clusters. In fact, from Table I it is clearly seen that the smaller the H-Si-nc, the longer is the difference between the absorption and HOMO-LUMO ground-state (GS) gap and between emission and HOMO-LUMO excited-state (EXC) gap.[37] In particular the GS HOMO-LUMO gap tends to be smaller than the absorption energy while the EXC HOMO-LUMO gap tends to be larger than the emission energy. In conclusion, trying to deduce the Stokes shift simply from the HOMO-LUMO gaps leads to not negligible errors which are more significant for smaller clusters.

When comparing our results for the ground state with other DFT calculations we note that there is a general good agreement between them. In particular, for Si_1H_4 Grossman *et al.*[18] have found 7.8 eV for the HOMO-LUMO gap while Onida and Andreoni[12] have obtained 8.1 eV; these values have to be compared with our calculated 7.93 eV result. At the same time, for the $Si_{29}H_{36}$ cluster, our 3.65 eV calculated absorption gap is in good agreement with the 3.6 eV (Ref. 38) obtained with the same method both by Puzder *et al.*[14] and Franceschetti *et al.*[29] It is worth mentioning that our results for the absorption gaps of the Si_1H_4 and Si_5H_{12} clusters agree quite well with the experimental results of Itoh *et al.*[39] whose excitation energies are 8.8 eV and 6.5 eV, respectively. *GW* calculations find an absorption gap of 9.0 eV for Si_1H_4,[19] while LDA results by Hirao *et al.*[40] show a HOMO-LUMO gap of 4.62 eV and 3.32 eV for $Si_{10}H_{16}$ and $Si_{29}H_{36}$, respectively. All these data are in very good agreement with ours.

Regarding the Stokes shift, really few theoretical results exist in literature as Table II shows,[14,29,41] and, in particular for really small H-Si-nc (from Si_1H_4 to $Si_{10}H_{16}$), no theoretical results exist. The dependence of the Stokes shift from the H-Si-nc size qualitatively agrees with the calculations of Puzder *et al.*[14] and Franceschetti *et al.*[29] Nevertheless, it is seen that the data for the $Si_{29}H_{36}$ cluster show a large spread, which can be attributed to the different approaches used, DFT-GGA in our case, a DFT-LDA in the case of Hirao[41] (with a very low cutoff of 6.6 Ry), Puzder *et al.*, and Franceschetti *et al.* It is worth pointing out that a large discrepancy is observed even between the last two calculations just cited, although both include local spin density approximation for the study of the excited electronic configuration (triplet configuration).

Experimentally, very few measurements exist on hydrogenated Si cluster and what emerges is a decrease of the Stokes shift value with increasing the clusters dimension.[42,43]

A last point must be stressed here. Recent results concerning optical gain in silicon nanoclusters embedded in a SiO_2 matrix have been described within a four-level, rate equation model.[22,23,44,45] In that case the presence of oxygen can induce localized states within the nanocrystals gap[15,46–48] making the electronic spectrum more complex. Anyway, the presence of the Stokes shift as depicted above can still give a possible interpretation concerning the nature of the levels invoked by the model. They can be identified with the HOMO and LUMO states in the ground- and excited-state configuration. Starting from a silicon nanocluster in its ground state, the pumping mechanism induces the HOMO-LUMO transition followed by a structural relaxation which leads to a more favorable geometrical arrangement of the atoms. This modifies the band edges, giving rise to new, differently localized HOMO and LUMO states now involved in the emission process. Thus, once more three fundamental aspects come out. First, there is a strong interplay between structural and electronic properties, mostly when excited configurations are concerned. Second, a consistent explanation of emission processes can be carried out only if such excited configurations are accounted for. Third, optical gaps cannot be calculated simply as the HOMO-LUMO energy

TABLE I. Calculated values for the absorption and ground state HOMO-LUMO energy gaps, the emission and excited HOMO-LUMO gaps, and Stokes shifts for the Si_1H_4, Si_5H_{12}, $Si_{10}H_{16}$, $Si_{29}H_{36}$, and $Si_{35}H_{36}$ clusters.

	Absorption gap (eV)	Ground state HOMO-LUMO gap	Emission gap (eV)	Excited state HOMO-LUMO gap	Stokes shift (eV)
Si_1H_4	8.76	7.93	0.38	1.84	8.38
Si_5H_{12}	6.09	5.75	0.42	0.46	5.67
$Si_{10}H_{16}$	4.81	4.71	0.41	0.55	4.40
$Si_{29}H_{36}$	3.65	3.58	2.29	2.44	1.35
$Si_{35}H_{36}$	3.56	3.50	2.64	2.74	0.92

separation without inducing errors which are larger for smaller clusters.

V. SOME CONSIDERATIONS ABOUT SYMMETRIES

For all the studied clusters the ground-state geometry has the T_d symmetry. This has been verified performing the optimization in two separate ways: in the first one the T_d symmetry has been imposed, while in the second one the atomic positions have been slightly randomized in order to relax the symmetry constraint. The result is that there is not any appreciable difference in the final atomic positions as well as in the total energy between the two cases. This cannot remain true when the relaxation is done in an excited state configuration. The electron-hole pair creation induces occupation of high-energy levels, breaking the ground-state symmetry. The optimization has to be carried out without any constraint on the symmetry in order to prevent the relaxation from falling into local energy minima.

Some previous calculations have been done without considering the influence that the symmetry of the structure has on the nanosystem electronic and optical properties.[17,24] In order to clearly show this point, two different calculations for the excited-state configuration both keeping and breaking the T_d symmetry of the ground state have been carried out. As an example we compare, in Fig. 9, the geometries obtained in the excited-state configuration when we keep (open circles) or relax (dark circles) the T_d symmetry of the $Si_{10}H_{16}$ cluster. The calculated Si-Si distances for each pair of Si atoms reported here for both the cases show how the constraint on the symmetry prevents the cluster from relaxation.

It is interesting to observe that the atomic positions of both the ground and excited states for a cluster with T_d symmetry are almost the same, whereas this does not occur when the excited cluster is relaxed without the T_d symmetry [see Fig. 3(c)]. Similarly, the calculated Kohn-Sham levels for the excited states reproduces the ground-state spectrum when the symmetry constraint is not relaxed. Finally, in Fig. 10 we show the HOMO and LUMO square modulus contour plots calculated for the $Si_{10}H_{16}$ cluster in the excited-state T_d configuration. Again, a result very similar to the ground state [see Fig. 7(b)] is found. We can therefore conclude that both energy levels and the resulting charge distribution for the T_d excited cluster practically do not change with respect to the ground state. These findings show how the electronic and geometrical properties obtained keeping the symmetry constraint for the excited state are far from being those at the actual energy minimum.

VI. FORMATION ENERGIES

The stability of silicon nanoclusters exposed to hydrogen atmosphere can be studied looking at formation energies as a function of the size. The interest in this kind of calculations consists in the understanding of which clusters are more likely to form under different growth conditions. A typical example is given by the $Si_{29}H_{24}$ cluster, which has been recently proposed[25,26,49] as a structural prototype of ultrasmall ultrabright stable particles and for this reason it has been considered here. This cluster is obtained from $Si_{29}H_{36}$ by

TABLE II. Stokes shift values for hydrogenated Si clusters: present work vs theoretical results present in literature.

H-Si Clusters	Diameter (nm)	This work	Ref. 14		Ref. 29	Ref. 41
Si_1H_4	0.0	8.38				
Si_5H_{12}	0.45	5.67				
$Si_{10}H_{16}$	0.55	4.40	LDA	QMC	LSDA	LDA
$Si_{29}H_{36}$	0.9	1.35	0.69	1.0	2.92	0.22
$Si_{35}H_{36}$	1.1	0.92	0.57	0.8		
$Si_{66}H_{64}$	1.3		0.50			
$Si_{87}H_{76}$	1.5		0.22		0.32	
$Si_{29}H_{24}$	0.8	0.84	0.34	0.4		

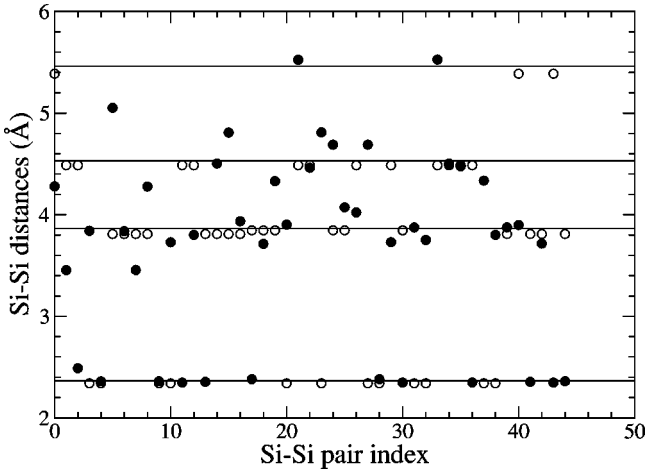

FIG. 9. Calculated Si-Si distances of each pair of Si atoms of the $Si_{10}H_{16}$ cluster in the excited state configuration with (open circles) and without (dark circles) the T_d symmetry constraint. Straight lines represent calculated bulk silicon values for the first, second, third, and fourth neighbors.

simply removing 12 hydrogens in a way so as to induce a surface reconstruction.

The stability of each cluster can be evaluated calculating the formation enthalpy (F) through the formula:

$$F(Si_NH_M) = E_{TOT}(Si_NH_M) - N\mu_{Si} - M\mu_H, \qquad (1)$$

where E_{TOT} is the ground-state total energy of a given Si_NH_M cluster, μ_{Si} and μ_H the chemical potentials for silicon and hydrogen, respectively.

The chemical potential for silicon (μ_{Si}) is fixed at the bulk value which is $\mu_{Si} = -107.802$ eV, while the chemical potential for hydrogen changes to simulate different growth conditions. Figure 11 shows the phase diagram of the clusters with respect to different conditions in the H atmosphere. All the possible values for μ_H we have considered have been referred to the calculated molecular hydrogen chemical potential which is $\mu_H = -15.656$ eV. Thus, $\Delta\mu_H = 0$ corresponds to the situation where the clusters are exposed to molecular hydrogen at T = 0 °K, negative values of $\Delta\mu_H$ correspond to a H-poor atmosphere in the growth chamber, positive values of $\Delta\mu_H$ mean that also atomic H is available (H-rich conditions). All the considered clusters are passivated by H atoms placed along the bulk silicon crystal directions except for the $Si_{29}H_{24}$ structure, as pointed out above. The surface reconstruction induces in this case the formation of Si-Si dimers. As expected, the $Si_{29}H_{24}$ structure, when compared with $Si_{29}H_{36}$, is stabler in H-poor growth conditions (not visible in Fig. 11), less stable in H-rich atmosphere. The exposure to molecular hydrogen or to a H-poor atmosphere gives higher stability to smaller clusters, while in H-rich growth conditions larger clusters are stabler. For clarity, the results obtained considering the exposure to molecular hydrogen at T = 0 °K are reported in Table III ($\Delta\mu_H = 0$ in Fig. 11). On increasing the H concentration (that is, moving from left to right in Fig. 11) the stablest cluster changes from Si_1H_4 to Si_5H_{12} and, finally, to $Si_{35}H_{36}$.

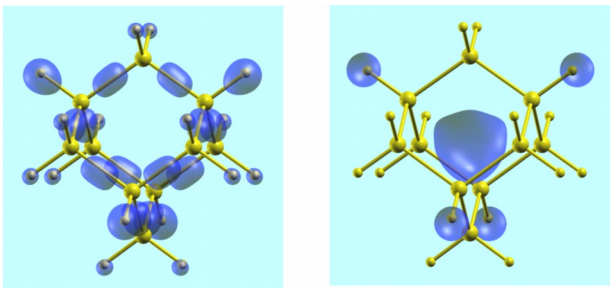

FIG. 10. (Color online) The HOMO (left) and LUMO (right) square modulus contour plots for the $Si_{10}H_{16}$ cluster in the excited-state configuration. The original T_d symmetry of the cluster has been kept during relaxation [see similarity with Fig. 7(b)]. The isosurfaces correspond to 25% of the maximum value. The HOMO is threefold degenerate and the shown charge density is the sum over the three states.

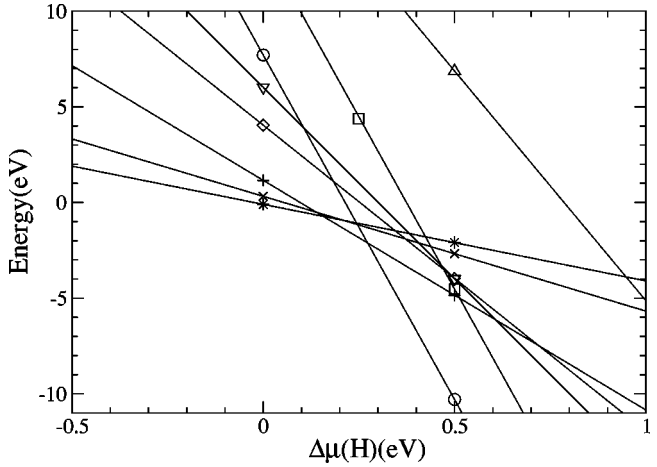

FIG. 11. Calculated phase diagram of the hydrogen exposed Si_1 (stars), Si_2 (crosses x), Si_5 (crosses +), Si_{10} (diamonds), Si_{14} (down triangles), Si_{29} ($Si_{29}H_{24}$ up triangles and $Si_{29}H_{36}$ squares) and Si_{35} (circles) clusters. The chemical potential of hydrogen, μ_H, is given with respect to molecular hydrogen.

VII. CONCLUSIONS

In this paper an investigation of the optical and electronic properties of hydrogenated silicon nanoclusters has been car-

TABLE III. Calculated ground state total energy and formation enthalpy for the SiH_4, Si_2H_6, Si_5H_{12}, $Si_{10}H_{16}$, $Si_{14}H_{20}$, $Si_{29}H_{24}$, $Si_{29}H_{36}$, and $Si_{35}H_{36}$ clusters in presence of molecular hydrogen.

	Ground state total energy (eV)	Formation enthalpy $F(Si_NH_M)$ (eV)
Si_1H_4	−170.52	−0.096
Si_2H_6	−309.21	0.32
Si_5H_{12}	−725.72	1.16
$Si_{10}H_{16}$	−1324.47	4.04
$Si_{14}H_{20}$	−1816.32	6.02
$Si_{29}H_{24}$	−3483.11	13.48
$Si_{29}H_{36}$	−3676.38	7.71
$Si_{35}H_{36}$	−4328.96	18.87

ried out. A systematic analysis of the structural properties reveals that the average Si-Si bond approaches the bulk bond length as the cluster dimension increases. This is not true for the individual distances, because of the presence of the surface and the hydrogen passivation. In particular, it has been shown that moving from the center of the cluster toward the surface a contraction of the outer Si shells is observed. Moreover, the effect on the cluster geometry due to the creation of an electron-hole pair (electron excitation from HOMO to LUMO) has been studied, showing how the charge density change induces significant distortions. A strong interplay between the nanocluster structural and electronic properties comes out. Such distortions modify the absorption and emission energies that, as pointed out, cannot be calculated simply as the HOMO-LUMO energy separation, and induce the presence of new localized energy levels. This can explain the Stokes shift as well as provide a possible four-level scheme able to account for optical gain in silicon nanoclusters. The role of the cluster symmetries, in calculating excited state properties has been pointed out, showing how the constraint on the symmetry prevents the cluster from relaxing with respect to the ground-state geometry. This leads to wrong geometry and charge density, as the comparison of Figs. 8(b) and 10 clearly show. Just to give an indication, when such constraint is relaxed for $Si_{10}H_{16}$, a total energy lowering of 0.044 Ha is obtained.

Finally, we calculated the formation energies for clusters ranging from 1 to 35 Si atoms. The phase diagram shows that increasing the H concentration the size of the stablest cluster increases from Si_1H_4 to Si_5H_{12} and finally to $Si_{35}H_{36}$.

ACKNOWLEDGMENTS

Financial support by INFM-PRA RAMSES, INFM-PAIS CELEX, and MIUR COFIN-PRIN 2002 is acknowledged. All the calculations have been performed at CINECA-Bologna (thanks to the ''Iniziativa Calcolo Parallelo dell'INFM'') and CICAIA-Modena advanced computing facilities.

[1] A.D. Yoffe, Adv. Phys. **50**, 1 (2001), and references therein.
[2] G. Cantele, G. Piacente, D. Ninno, and G. Iadonisi, Phys. Rev. B **66**, 113308 (2002).
[3] A. Zunger, Phys. Status Solidi B **224**, 727 (2001).
[4] R.J. Baierle, M.J. Caldas, E. Molinari, and S. Ossicini, Solid State Commun. **102**, 545 (1997).
[5] Y.M. Niquet, C. Delerue, G. Allan, and M. Lannoo, Phys. Rev. B **62**, 5109 (2000).
[6] L.W. Wang and A. Zunger, J. Phys. Chem. **98**, 2158 (1994).
[7] B. Delley and E.F. Steigmeier, Appl. Phys. Lett. **67**, 2370 (1995).
[8] L. Dorigoni, O. Bisi, F. Bernardini, and S. Ossicini, Phys. Rev. B **53**, 4557 (1996).
[9] E. Degoli, M. Luppi, and S. Ossicini, Phys. Status Solidi A **182**, 301 (2000).
[10] E. Degoli and S. Ossicini, Surf. Sci. **470**, 32 (2000).
[11] A.N. Kholod, S. Ossicini, V.N. Borisenko, and F. Arnaud D'Avitaya, Surf. Sci. **527**, 30 (2003).
[12] G. Onida and W. Andreoni, Chem. Phys. Lett. **243**, 183 (1995).
[13] A.J. Williamson, J.C. Grossman, R.Q. Hood, A. Puzder, and G. Galli, Phys. Rev. Lett. **89**, 196803 (2002).
[14] A. Puzder, A.J. Williamson, J.C. Grossman, and G. Galli, J. Am. Chem. Soc. **125**, 2786 (2003).
[15] M. Luppi and S. Ossicini, J. Appl. Phys. **94**, 2130 (2003).
[16] I. Vasiliev, S. Öğüt, and J.R. Chelikowsky, Phys. Rev. Lett. **86**, 1813 (2001).
[17] C.S. Garoufalis, A.D. Zdetsis, and S. Grimme, Phys. Rev. Lett. **87**, 276402 (2001).
[18] J.C. Grossman, M. Rohlfing, L. Mitas, S.G. Louie, and M.L. Cohen, Phys. Rev. Lett. **86**, 472 (2001).
[19] M. Rohlfing and S.G. Louie, Phys. Rev. Lett. **80**, 3320 (1998).
[20] R.W. Godby and I.D. White, Phys. Rev. Lett. **80**, 3161 (1998); A. Franceschetti, L.W. Wang, and A. Zunger, *ibid.* **83**, 1269 (1999).
[21] C. Delerue, M. Lannoo, and G. Allan, Phys. Rev. Lett. **84**, 2457 (2000).
[22] L. Pavesi, L. Dal Negro, C. Mazzoleni, G. Franzò, and F. Priolo, Nature (London) **408**, 440 (2000).
[23] L. Dal Negro, M. Cazzanelli, L. Pavesi, S. Ossicini, D. Pacifici, G. Franzò, F. Priolo, and F. Iacona, Appl. Phys. Lett. **82**, 4636 (2003).
[24] H.-C. Weissker, J. Furthmüller, and F. Bechstedt, Phys. Rev. B **67**, 245304 (2003).
[25] L. Mitas, J. Therrien, R. Twesten, G. Belomoin, and M.H. Nayfeh, Appl. Phys. Lett. **78**, 1918 (2001).
[26] G. Belomoin, E. Rogozhina, P.V. Braun, L. Abuhassan, M.H. Nayfeh, L. Wagner, and L. Mitas, Phys. Rev. B **65**, 193406 (2002).
[27] First-principles computation of material properties: the ABINIT software project (http://www.abinit.org). X. Gonze, J.-M. Beuken, R. Caracas, F. Detraux, M. Fuchs, G.-M. Rignanese, L. Sindic, M. Verstraete, G. Zerah, F. Jollet, M. Torrent, A. Roy, M. Mikami, Ph. Ghosez, J.-Y. Raty, and D.C. Allan, Comput. Mater. Sci. **25**, 478 (2002).
[28] It should be noted that similar calculations have been done by Franceschetti and Pantelides[29] within local spin-density approximation, showing that the singlet-triplet splitting is significantly smaller than the Stokes shift.
[29] A. Franceschetti and S.T. Pantelides, Phys. Rev. B **68**, 033313 (2003).
[30] V. Meleshko, Yu. Morokov, and V. Schweigert, Chem. Phys. Lett. **300**, 118 (1999).
[31] H.-C. Weissker, J. Furthmüller, and F. Bechstedt, Phys. Rev. Lett. **90**, 085501 (2003).
[32] Similar results concerning the average bond length in Ge nanoparticles have been shown in L. Pizzagalli, G. Galli, J.E. Klepeis, and F. Gygi, Phys. Rev. B **63**, 165324 (2001).
[33] The $Si_{29}H_{36}$ cluster is built up starting from a Si atom and adding Si shells up to the third neighbors (the surface dangling bonds are passivated with H atoms). The starting Si atom will be referred to as the ''central'' one.
[34] Also in this case, starting from the distorted excited state geom-

etry and going back down to the ground state the systems relax again to the initial T_d symmetric configuration.

[35] A. Kokalj, J. Mol. Graphics Modell. **17**, 176 (1999).

[36] O. Bisi, S. Ossicini, and L. Pavesi, Surf. Sci. Rep. **38**, 5 (2000).

[37] We note from Table I that, in our calculations, on going from smaller to large clusters the difference between the HOMO-LUMO gap in the ground state and the absorption gap becomes smaller and smaller. Recently Delerue *et al.*,[21] have pointed out that for clusters with diameter larger than 1.2 nm there is a cancellation between self-energy correction and Coulomb term. Thus, the lowest excitonic energy is ''correctly'' predicted by the single-particle theories with the bulk correction for the gap. Delerue result anyway cannot be applied to our case because of the dimension of our clusters; they are smaller with respect to Delerue's ones.

[38] The absorption gap value for the $Si_{29}H_{36}$ cluster cited by Franceschetti is 4.3 eV but it is estimated by adding the local-spin density band gap error of bulk Si (0.7 eV).

[39] U. Itoh, Y. Toyoshima, H. Onuki, N. Washida, and T. Ibuki, J. Chem. Phys. **85**, 4867 (1986).

[40] M. Hirao and T. Uda, Surf. Sci. **306**, 87 (1994).

[41] M. Hirao, in *Microcrystalline and Nanocrystalline Semiconductors*, edited by L. Brus, M. Hirose, R. W. Collins, F. Koch, and C. C. Tsai, Mater. Res. Soc. Symp. Proc. 358 (Materials Research Society, Pittsburgh, 1995).

[42] G. Belomoin, J. Therrien, A. Smith, S. Rao, R. Twesten, S. Chaieb, M.H. Nayfeh, L. Wagner, and L. Mitas, Appl. Phys. Lett. **80**, 841 (2002).

[43] Y. Kanemitsu and S. Okamoto, Phys. Rev. B **58**, 9652 (1998).

[44] S. Ossicini, C. Arcangeli, O. Bisi, E. Degoli, M. Luppi, R. Magri, L. Dal Negro and L. Pavesi, in *Toward the First Silicon Laser*, Vol. 93, *NATO Advanced Studies Institute*, Series II, edited by L. Pavesi, S. Gaponenko, and L. Dal Negro (Kluwer, Academic, Dordrecht, 2003), p. 261.

[45] L. Dal Negro, M. Cazzanelli, N. Daldosso, Z. Gaburro, L. Pavesi, F. Priolo, D. Pacifici, G. Franzò, and F. Iacona, Physica E (Amsterdam) **16**, 297 (2003).

[46] M. Luppi and S. Ossicini, Phys. Status Solidi A **197**, 251 (2003).

[47] N. Daldosso, M. Luppi, S. Ossicini, E. Degoli, R. Magri, G. Dalba, P. Fornasini, R. Grisenti, F. Rocca, L. Pavesi, S. Boninelli, F. Priolo, C. Spinella, and F. Iacona, Phys. Rev. B **68**, 085327 (2003).

[48] M.V. Wolkin, J. Jorne, P.M. Fauchet, G. Allan, and C. Delerue, Phys. Rev. Lett. **82**, 197 (1999).

[49] E.W. Draeger, J.C. Grossman, A.J. Williamson, and G. Galli, Phys. Rev. Lett. **90**, 167402 (2003).